The EMBO Journal vol.15 no.9 pp.2249–2255, 1996

Multiple substrate binding sites in the ribozyme from *Bacillus subtilis* RNase P

Tao Pan[1] and Monika Jakacka

Department of Biochemistry and Molecular Biology, University of Chicago, Chicago, IL 60637, USA

[1]Corresponding author

The ribozyme from *Bacillus subtilis* RNase P (P RNA) recognizes an RNA structure consisting of the acceptor stem and the T stem–loop of tRNA substrates. An *in vitro* selection experiment was carried out to obtain potential RNA substrates that may interact with the P RNA differently from the tRNA substrate. Using a P RNA-derived ribozyme that contains most, if not all, of the structural elements thought to be involved in active site formation of P RNA, but lacks the putative binding site for the T stem–loop of tRNA, a single RNA substrate was isolated after nine rounds of selection. This RNA is a competent substrate for the ribozyme used in selection as well as for the full-length P RNA. Biochemical characterization shows that this selected substrate interacts at a different site compared with the tRNA substrate. The selection experiment also identified a self-cleaving RNA seemingly different from other known ribozymes. These results indicate that a biological ribozyme can contain different binding sites for different RNA substrates. This alternate binding site model suggests a simple mechanism for evolving existing ribozymes to recognize RNA substrates of diverse structures.

Keywords: *in vitro* selection/ribozyme/RNA–RNA recognition/RNase P/tRNA

Introduction

RNA–RNA recognition plays a pivotal role in RNA catalysis. Although most biological reactions involving ribozymes do not occur with multiple turnover *in vivo*, they can often be converted into bimolecular reactions in which one RNA is designated as the enzyme that cleaves another RNA designated as the substrate (Cech, 1993; Long and Uhlenbeck, 1993). Small ribozymes, such as the hammerhead and the hairpin, recognize their substrates primarily through Watson–Crick base pairs to form one or more helices. Large ribozymes, such as group I intron or RNase P, can be designed to recognize their substrates through intermolecular Watson–Crick base pairing using a guide sequence that is either a part of the ribozyme (Cech, 1990) or a second RNA (Forster and Altman, 1990). Large ribozymes can also recognize the structure, rather than the sequence, of an RNA substrate. For example, the *Tetrahymena* group I ribozyme can be constructed *in vitro* to cleave a pre-formed RNA hairpin (Doudna and Szostak, 1989; Doudna and Cech, 1995).

Structure recognition of an RNA is used extensively by RNase P whose cellular functions include producing the mature 5′ end of tRNAs (Altman *et al.*, 1993; Pace and Brown, 1995). The RNA component of the bacterial RNase P (denoted P RNA) is active *in vitro* and it recognizes the acceptor stem and the T stem–loop regions of tRNA. These two stems coaxially stack to form a pseudo-continuous helix of 12 bp with conserved nucleotides at both ends. The end of this coaxially stacked helix containing the reactive phosphate is bound by the active site residues in several highly conserved regions of *Bacillus subtilis* P RNA (Haas *et al.*, 1994; Harris *et al.*, 1994; Westhof and Altman, 1994). Binding in this region is enhanced by interactions of the 3′ CCA in tRNA with loop L15 of P RNA (Kirsebom and Svard, 1994; La-Grandeur *et al.*, 1994; Oh and Pace, 1994). Identification of a specific interaction between a 2′ OH group in the T stem and P RNA (Pan *et al.*, 1995) together with P RNA–tRNA photocross-linking data (Nolan *et al.*, 1993; Harris *et al.*, 1994) suggest that the T stem–loop binding site is located primarily in the P7–P11 region of P RNA. Although the residues around the site of cleavage must fit into the active site, the T stem–loop, which extends 12–35 Å away from the reactive phosphate, may be substituted by another RNA structural motif. Such an RNA structural motif potentially can be recognized by P RNA either through interaction at the same site as the T stem–loop of tRNA or through interaction at a new site in the P RNA. Therefore, although the P RNA contains only a single active site, it may have more than one binding site to accommodate different substrates with distinct structures.

One possible clue for the alternate binding site hypothesis comes from the discovery and characterization of other biological substrates for RNase P (Peck-Miller and Altman, 1991; Komine *et al.*, 1994; Hartmann *et al.*, 1995). Some of these substrates, such as the 10Sa RNA, appear to contain RNA structures similar to the coaxially stacked T stem–loop and acceptor stem of tRNA. Other substrates, such as the 4.5S RNA, lack the conserved T loop structure at the corresponding position, suggesting that some of these substrates may interact with P RNA differently. Indeed, in the absence of the protein component of RNase P, deletion of nucleotides 92 or 185–201 in *Escherichia coli* P RNA had no relative effect on cleavage of a 4.5S RNA precursor, but caused a >1000-fold decrease in relative cleavage efficiency of a tRNA substrate, suggesting differences in the recognition elements of these two substrates (Talbot and Altman, 1994).

Support for this hypothesis was also obtained from identification of two classes of RNA substrates by *in vitro* selection (Pan, 1995b). Class I substrates contain a putative T stem–loop-like structure but lack the acceptor stem, whereas class II substrates have a putative acceptor stem-like structure but lack the T stem–loop. Thus, it is logical

© Oxford University Press

to suggest that some of the class II substrates may interact at a region in P RNA not involved in interactions with tRNA. Here we describe the isolation and characterization of an RNA substrate that interacts at a new site in the *B.subtilis* P RNA. Although the wild-type P RNA has comparable activity for the pre-tRNA and this new substrate, P RNA derivatives have been constructed that lack one or other site of interaction. These P RNA-based ribozymes are either inactive toward tRNA substrates but retain nearly full activity toward the selected substrate, or are fully active for tRNA substrates but have greatly diminished activity for the selected variant.

Results

Selection of RNA substrates using a P RNA derivative

In order to isolate RNA substrates that may bind at a site different from pre-tRNA, an RNA construct including nucleotides 240–401 + 1–61 of the *B.subtilis* P RNA [denoted p(240–61)] was used. This RNA contains the highly conserved residues in P RNA considered to form the active site, but is completely inactive toward pre-tRNA substrates (Pan, 1995a). This loss of activity is possibly due to elimination of the region in P RNA required for T stem–loop binding and/or deletion of nucleotides involved in forming the active site. If an RNA substrate can be isolated for p(240–61), the active site of P RNA should be confined within this molecule. In addition, this substrate may bind at a site distinct from the tRNA binding site.

An *in vitro* selection procedure was applied in which RNA substrates for p(240–61) can be obtained regardless of the location of the cleavage site (Pan and Uhlenbeck, 1992; Pan, 1995b). The selection protocol involves cleavage of a circular RNA library containing 70 randomized nucleotides. Active RNA substrates that are cleaved by p(240–61) become linear, while inactive RNAs that are not cleaved remain circular. The linear RNA products can then be separated easily from the circular RNAs on a denaturing gel. The linear RNAs are converted back into the circular form to allow cDNA synthesis and PCR amplification to produce a new RNA mixture enriched in substrates for p(240–61). When this procedure was used previously to isolate novel RNA substrates for the full-length *B.subtilis* P RNA, numerous substrates were identified (Pan, 1995b). These selected substrates are cleaved by P RNA with k_{cat}/K_m values up to 4-fold higher than that for a pre-tRNA^{Phe} substrate at 50 mM Tris, pH 8.1, 25 mM $MgCl_2$, 37°C. This previous selection experiment was carried out at 25 mM Mg^{2+} for the initial four rounds and then at 10 mM Mg^{2+} for the next four rounds, with the expectation that the activity of the selected substrates may be less sensitive to Mg^{2+} concentration. However, it was found later that the cleavage efficiencies of these substrates were decreased by 15- to 20-fold when the Mg^{2+} concentration was decreased from 25 to 10 mM, essentially identical to the Mg^{2+} sensitivity of the pre-tRNA^{Phe} (Pan, 1995b). It was then discovered that addition of 1 mM spermine at 10 mM $MgCl_2$ increased the k_{cat}/K_m of pre-tRNA^{Phe} by ~15-fold for *B.subtilis* P RNA (Table I) and ~50-fold for *E.coli* P RNA (T.Pan, unpublished results). Thus, spermine appears to have profound

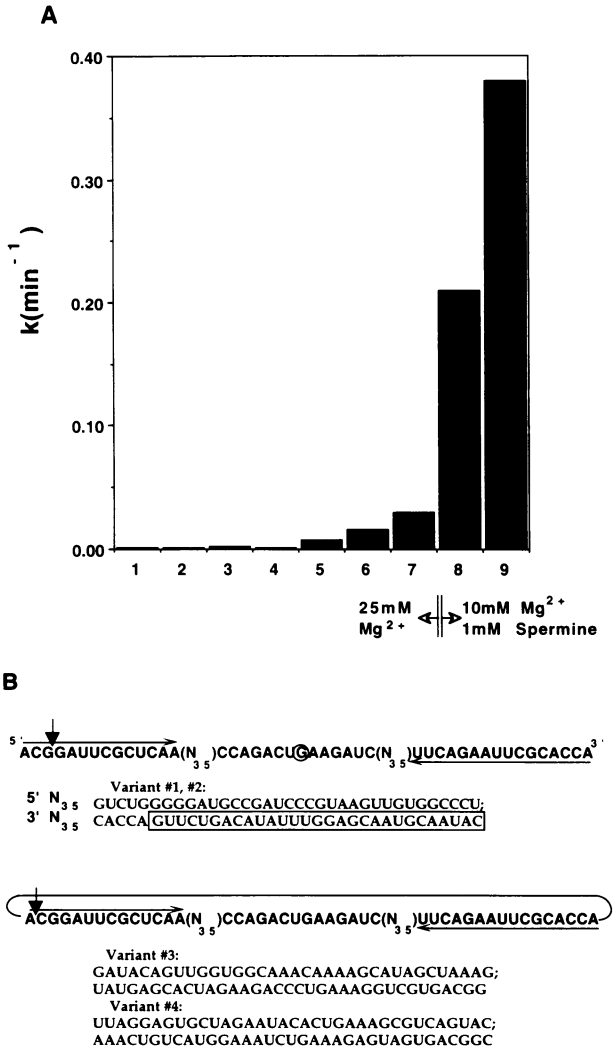

Fig. 1. (**A**) Enrichment of RNA substrates for p(240–61). Rounds 1–7 were carried out in 50 mM Tris, pH 8.1, 25 mM $MgCl_2$, and rounds 8 and 9 in 50 mM Tris, pH 8.1, 10 mM $MgCl_2$, 1 mM spermine, 37°C. The *y*-axis shows the rate of linearization of the circular RNA library. (**B**) Sequence of the randomized regions of the selected variants. The primer binding sites are indicated by horizontal arrows. The cleavage sites are indicated by vertical arrows. The 5′ and 3′ randomized regions are separated by a semicolon. The circled nucleotide in the constant region was changed to an A in variant #1. The boxed nucleotides in variants #1 and #2 can be deleted without affecting the cleavage activity. Variants #3 and #4 are shown in the circular form. Whether the linear form of #3 and #4 is also active remains to be determined.

effects on the cleavage activity of P RNA reactions and is included in the selection experiment using p(240–61).

The progressive enrichment of RNA substrates for p(240–61) is shown in Figure 1A. Only 25 mM $MgCl_2$ was included for the first seven rounds of selection. A detectable increase in cleavage activity was apparent after five rounds. However, no substantial improvement was observed for rounds 6 and 7. The cleavage efficiency of the RNA library was increased by 7-fold when 1 mM spermine was added at round 8, 2-fold more at round 9, but remained the same at round 10. The RNA library after nine rounds of selection was then cloned and 28 clones were sequenced (Figure 1B). Only four sequences were

Table I. Reactivity of the selected variants

Variant #[a]	k_{cat}/K_m [p(240–61)][b]	k_{cat}/K_m [p(240–61)]	k_{cat}/K_m (full-length P RNA)
#1 (13)	1.4 (circular) 1.5 (linear)	0.09 (circular)[c]	22 (circular) 25 (linear)
#2 (9)	0.7 (circular)	0.03 (circular)[c]	17 (circular)
Pre-tRNA^{Phe}	not detected	not detected[c]	4.4
Self-cleaving	k (per min)		
#3 (5)	0.03 (circular)		
#4 (1)	0.04 (circular)		

[a]The numbers in parentheses indicate the total number of identical clones from 28 sequences.
[b]All k_{cat}/K_m values (per μM/min) were determined under single turnover conditions using 30–60 nM p(240–61) or 10–30 nM full-length P RNA. In one instance [variant #1, linear, p(240–61)], the k_{cat} and K_m were measured to be 0.37/min and 0.24 μM, respectively. Unless otherwise indicated, all reactions were carried out at 50 mM Tris–HCl, pH 8.1, 10 mM $MgCl_2$, 1 mM spermine, 37°C.
[c]Conditions: 50 mM Tris–HCl, pH 8.1, 25 mM $MgCl_2$, 37°C.

present, with one variant (#2) having a sequence identical to variant #8 isolated from the previously reported selection experiment using full-length P RNA (Pan, 1995b). Variant #1 has the same sequence as variant #2 except a single G→A change in a region that was not randomized in the initial RNA library (Figure 1B). Variants #3 and #4 differ significantly from #1 and #2.

Characterization of selected variants

The cleavage activity of variants #1 and #2 in the circular and in the linear form was examined using trace amounts of ^{32}P-labeled variant with 60 nM p(240–61) (Table I). The linear RNA contains the normal 5′ end prior to ligation by RNA ligase. The apparent k_{cat}/K_m values for circular and linear forms of variant #1 differ by <20%, indicating that circularization has no effect on the cleavage efficiency. The difference between k_{cat}/K_m of variants #1 and #2 is only ~2-fold, suggesting that the G→A change does not affect the reactivity significantly. The location of the cleavage site was mapped using 5′ ^{32}P-labeled linear RNA and was found to be in the 5′ primer region, three nucleotides from the 5′ end (Figure 1B). This site is one nucleotide 3′ to the cleavage site of four class II substrates for full-length *B.subtilis* P RNA (Pan, 1995b), and p(240–61) has no detectable activity for these other class II substrates (data not shown). Addition of 1 mM spermine at 10 mM Mg^{2+} increased the cleavage efficiency by ~15-fold relative to 25 mM Mg^{2+} alone (Table I). If we assume that the Mg^{2+} dependence of variant #1 is comparable with the pre-tRNA^{Phe} substrate which exhibited a 15-fold reduction in k_{cat}/K_m from 25 to 10 mM Mg^{2+}, then the net effect of 1 mM spermine at 10 mM Mg^{2+} can be estimated to approach ~225-fold.

Both the circular and the linear variant #1 are also excellent substrates for the full-length *B.subtilis* P RNA (Table I). The location of the cleavage site for the reaction catalyzed by P RNA is identical to that for p(240–61). In both reactions, the cleavage products appear to contain a 5′ phosphate and a 3′ OH group, as indicated by the slower migration of the 5′ ^{32}P-labeled trimer product on a denaturing gel compared with the same trimer containing

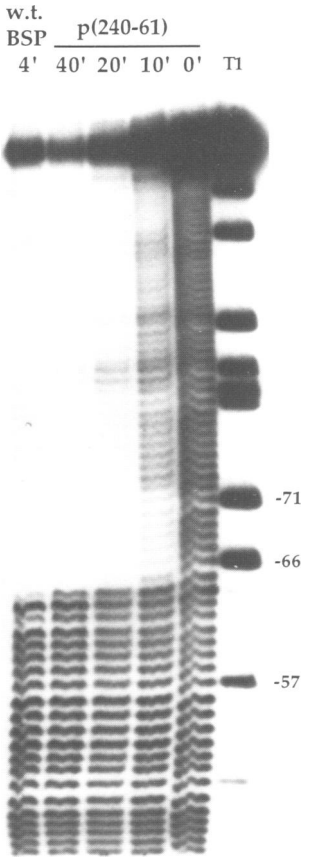

Fig. 2. Terminal truncation of variant #1 using p(240–61) (0.1 μM) and the full-length P RNA (w.t. BSP, 0.05 μM). The reaction time in minutes is indicated on the top of the gel. Residues numbers (beginning at +1 for the nucleotide 3′ to the cleavage site) as indicated by partial T1 digestion are shown at the right.

a 2′,3′ cyclic phosphate (data not shown). These results indicate that this substrate interacts with p(240–61) and P RNA at an identical site to position the reactive phosphate into the same active site. Thus, the majority, if not all, residues required to form the active site of P RNA are included in p(240–61).

Terminal truncation experiments were carried out to determine how many nucleotides can be deleted from the 3′ end of variant #1 without affecting the cleavage activity. When the 5′ ^{32}P-labeled variant is subjected to partial alkaline hydrolysis followed by cleavage, active fragments of this variant are cleaved and the ^{32}P-label transferred to the 5′ trimer product. Figure 2 shows that 45 nucleotides can be deleted from the 3′ end using either p(240–61) or full-length P RNA in the reaction. This result further confirms that variant #1 is recognized identically by both ribozymes.

Remarkably, cleavage of the circular form of variants #3 and #4 was independent of the presence of p(240–61) (Table I). The only requirement for the cleavage of these variants is the presence of 10 mM Mg^{2+} and 1 mM spermine. The cleavage site of circular variants #3 and #4 is located one nucleotide 3′ to the site of ligation by RNA ligase (Figure 1B). Thus, variants #3 and #4 are self-cleaving RNAs selected by this procedure.

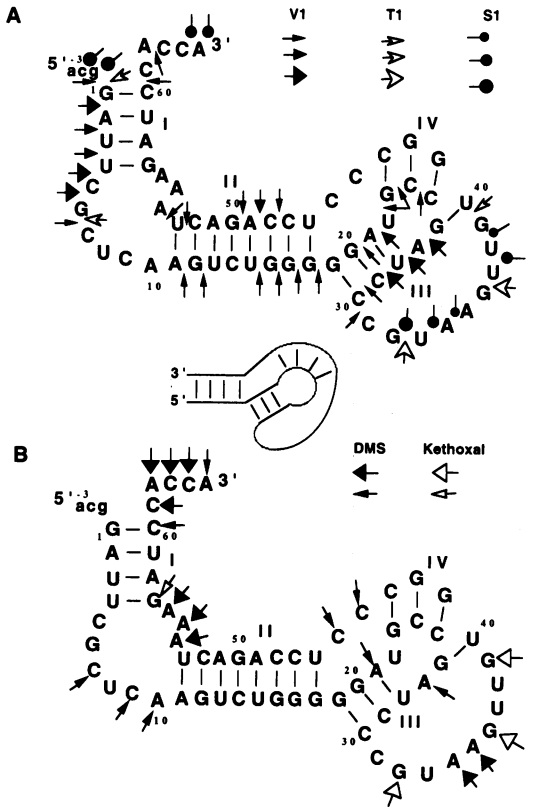

Fig. 3. Structural mapping of variant #1 using nucleases V1, T1 and S1 (**A**) or chemical reagents DMS and kethoxal (**B**). Only the 5′ 68 nucleotides are shown. The three residues 5′ to the cleavage site are shown in lower case. The size of the arrows corresponds to the extent of cleavage by nuclease or modification by chemicals. For clarity, a schematic diagram of the phosphate backbone is also drawn for residues 15–49.

Secondary structure of variant #1

A proposed secondary structure of variant #1 was confirmed by nuclease mapping and chemical modification (Figures 3 and 4). The secondary structure consists of three helical stems, I–III, and one pseudoknot, stem IV (Figure 3). The single nucleotide difference among variants #1 and #2 resides in an internal loop between stems I and II. The structure near the cleavage site is reminiscent of the structure around the cleavage site in tRNA substrates. Since cleavage of variant #1 also requires the 3′ CCA nucleotides (residues 63–65), this part of the selected substrate is likely to be recognized in a way similar to the corresponding region in tRNA substrates. For example, the 3′ CCA binding site in loop L15 of *B.subtilis* P RNA (Kirsebom and Svard, 1994; LaGrandeur *et al.*, 1994) may also be utilized to bind the 3′ CCA of variant #1.

The most significant difference between the selected and the tRNA substrate appears to be the lack of a T stem–loop structure. This is hardly surprising since the corresponding region in P RNA (P7–P11, nucleotides 86–134 + 175–181 + 230–239) which is likely to interact with the T stem–loop of tRNA is absent in p(240–61). The function of the T stem–loop in tRNA substrates may be substituted by the pseudoknot structure consisting of stems III, IV and a single-stranded region of residues 31–39 (Figure 3). Sequence inspection shows that residues 32–37 in the selected variant, 5′ GUAAGU, are complementary to residues 398–403, 5′ ACUUAC, in loop L1 in p(240–61) and in the 3′ overhanging region of the full-length P RNA. Since these residues are not involved in the secondary structure, they have the potential to form Watson–Crick base pairs in the structural context of these RNAs. To test this possibility, a variant form of *B.subtilis* P RNA was synthesized in which residues 398–403 (six nucleotides) were changed to 5′ CAGU 3′ (three identical nucleotides plus one mismatch). This P RNA mutant has identical cleavage activity toward the pre-tRNA^{Phe} substrate, but has a k_{cat}/K_m reduced by ~65-fold for variant #1. When the sequence of L1 in p(240–61) (5′ ACCACUUACAU$_3$G$_3$AUC, nucleotides 398–403 underlined) was changed to a GA$_3$ tetraloop (5′ ACGA$_3$GU), no detectable activity was observed for variant #1 (data not shown). These results strongly suggest that the loop L1 in p(240–61) constitutes a part of the binding site for the selected variant, but makes no contact with pre-tRNA substrates.

Discussion

We have described the isolation and characterization of a novel RNA substrate that binds at a different site in *B.subtilis* P RNA. Although $>10^{13}$ molecules were present in the initial RNA pool, a single RNA substrate was found after nine rounds of selection using a P RNA-derived ribozyme lacking part of the tRNA binding site. When the selection was carried out using full-length P RNA, a minimum of 14 different RNA substrates were selected after eight rounds (Pan, 1995b). However, all but one of these 14 variants are inactive for p(240–61) (T.Pan, unpublished results), suggesting that the activity of these other previously selected substrates requires the part of P RNA absent in p(240–61).

The function of this new RNA binding site can be best understood by considering the structure of the selected and the tRNA substrates as two RNA motifs connected by a helical stem (Figure 5). In tRNA, one motif consists of the reactive phosphate at the 5′ end of the acceptor stem with the 3′ CCA (cleavage site or CS motif), whereas the other motif contains the T stem with the highly conserved T loop nucleotides (T stem–loop or TSL motif). In variant #1, one motif consists of the reactive phosphate with the selected 3′ CCA (CS motif), whereas the other motif is the pseudoknot structure with a single-stranded loop of nine nucleotides (pseudoknot/loop or PL motif). Stem II in variant #1 probably serves as the helical connector between these motifs. This connector in tRNA is composed of the 3′ half of the acceptor stem coaxially stacked with the 5′ half of the T stem.

The CS motifs in variant #1 and pre-tRNA are similar in structure and spatial arrangement of the 3′ CCA nucleotides to the reactive phosphate. It is plausible that CS motifs in both substrates are bound at the same site in P RNA and might form identical intermolecular interactions for recognition. The P RNA binding site for this motif is likely to include conserved nucleotides considered to form the active site as well as the L15 residues which interact with the 3′ CCA of tRNA (Harris *et al.*, 1994; Westhof and Altman, 1994). Perhaps this binding site has evolved to accommodate the CS motif of tRNA so that there is selection pressure for the same RNA

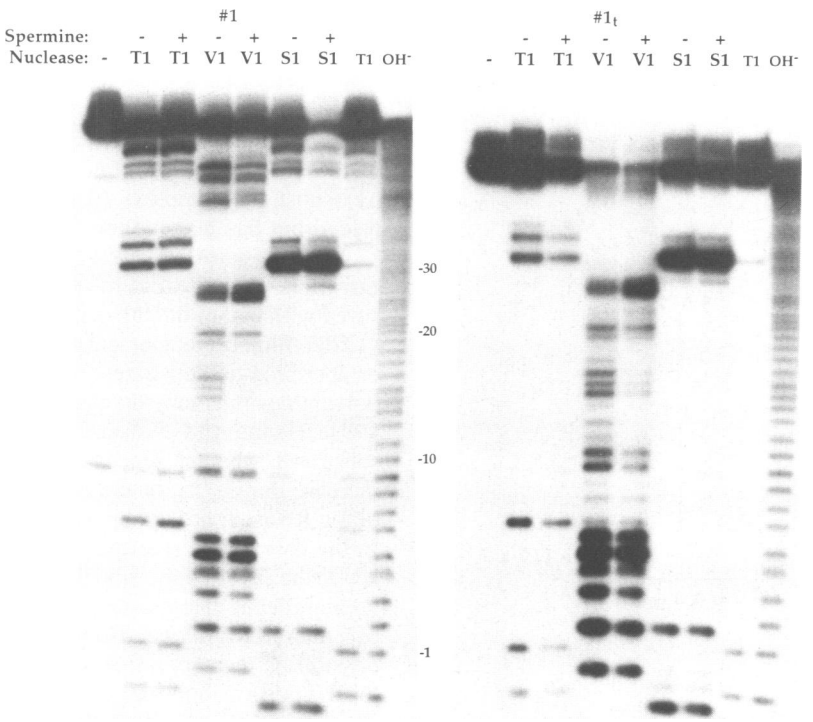

Fig. 4. Structural mapping of variant #1 and an RNA containing only the 5′ 68 nucleotides of this variant (#1_t). #1_t contains two inadvertent mutations of A54→G and G57→A. The k_{cat}/K_m of #1_t is within 2-fold that of the full-length variant #1. The identical pattern of nuclease digestion indicates that the 5′ 68 nucleotides form the same structure without the remainder of the molecule, consistent with the terminal truncation data.

structure in another substrate. Whether the difference between the cleavage site of variant #1 and pre-tRNA by one nucleotide plays an important role in CS motif recognition remains to be determined. It would be interesting to use a variant form of P RNA containing an altered binding site for the CS motif, e.g. converting L15 into a GNRA tetraloop to select for altered CS motifs in other RNA substrates.

The second structural motif involved in P RNA binding differs significantly between the selected and the tRNA substrates. One contact site in the PL motif is the loop containing nucleotides 31–39, as suggested by several lines of evidence. (i) Nucleotides 32–37 are complementary to the unpaired nucleotides 398–403 in p(240–61). (ii) Nuclease mapping of variant #1 indicates that this loop is fully accessible for direct interactions. (iii) A P RNA lacking a part of this complementary sequence shows significantly reduced activity for the selected substrate, although this deletion has no effect on its activity for the tRNA substrate. (iv) A p(240–61) derivative with substitutions in loop L1 has no detectable activity (>1000-fold less active) for the selected substrate. Watson–Crick base pairing plus 3′ stacking between these complementary nucleotides can provide up to –6.3 kcal/mol in free energy after subtracting 3.2 kcal/mol for bimolecular association (Turner *et al.*, 1988; Wyatt *et al.*, 1990). If we assume that K_m of this substrate (0.24 μM) is of the same magnitude as the binding constant, these interactions can provide up to two-thirds of the free energy needed for specific binding. The pseudoknot structure is also required, presumably to present these base-paring nucleotides in the correct structural context. This is indicated by the observation that breakage of many phosphodiester bonds in the pseudoknot structure results in a >10-fold decrease in cleavage efficiency (T.Pan, unpublished results). The binding site for the PL motif appears to involve mostly the loop L1 in p(240–61) or the corresponding 3′ overhanging nucleotides in the full-length P RNA (Figure 5). For the other structural elements in p(240–61) whose functions have not yet been assigned, L15.1 is likely to interact intramolecularly with P5.1 (nucleotides 62–80) in the full-length P RNA (Pan, 1995a) and hence is unlikely to be involved directly in binding. Whether P3, P18 and P19 are used in some way to contact the selected substrate remains to be seen.

The binding site for the TSL motif in tRNA appears to be located in the region consisting of P7–P11 in the P RNA (Harris *et al.*, 1994; Westhof and Altman, 1994). One direct contact between tRNA substrate and the P RNA involves the 2′ OH group of residue 62 in the T stem with the conserved A230 in *B.subtilis* P RNA (Pan *et al.*, 1995). Other ribozyme–substrate interactions involving the T stem–loop have not yet been identified. The structural integrity of this motif for the cleavage efficiency is clearly important, as indicated by circular permutation analysis of a pre-$tRNA^{Phe}$ substrate (Pan *et al.*, 1995). Since most of the highly conserved T loop nucleotides are involved in tertiary folding of tRNA, it is unlikely that T loop binding is supported by forming an intermolecular helix. Therefore, the TSL motif not only binds at a different site in P RNA, but the nature of ribozyme–substrate interaction is likely to be distinct from that of the PL motif in the selected substrate.

The ability of p(240–61) and full-length P RNA to generate the same cleavage products suggests that most, if not all, residues of the P RNA active site are confined

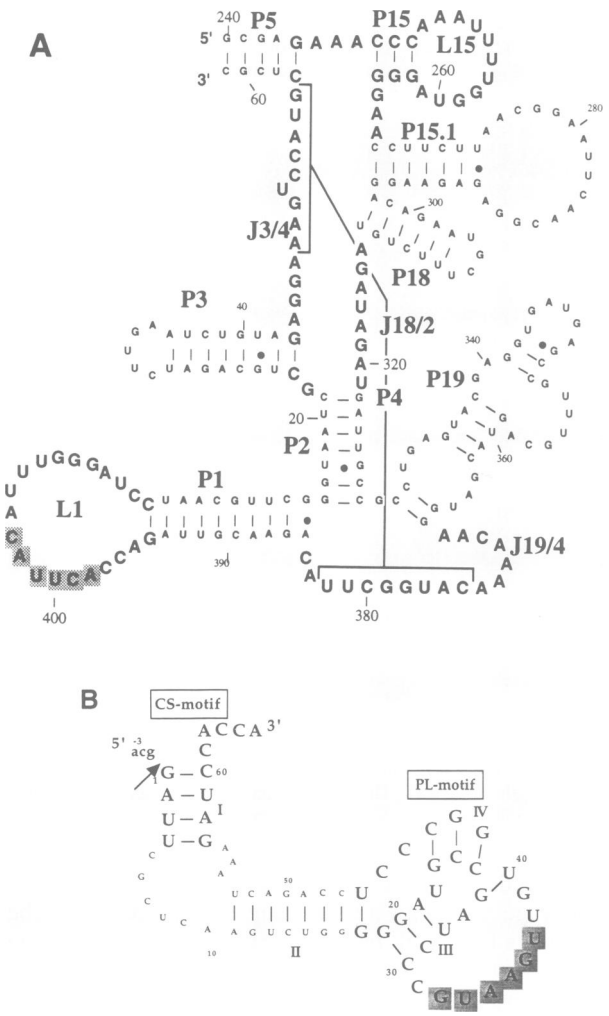

Fig. 5. (**A**) The secondary structure of p(240–61) with the putative binding sites for variant #1 shown in large font. Loop L1 contains residues of natural *B.subtilis* P RNA (up to 401) plus six extra nucleotides from the cloning vector designated as 402–407. The active site residues plus the 3′ CCA binding site (L15) bind the CS motif, whereas loop L1 binds the PL motif. Nucleotides 398–403 that are complementary to nucleotides 32–37 in variant #1 are shaded. (**B**) The secondary structure of the 5′ 68 nucleotides of variant #1. The CS motif and the PL motif are separated by a putative linker region shown in smaller font. Nucleotides 32–37 are shaded. The cleavage site is indicated by an arrow.

within p(240–61) which contains approximately one-half of all P RNA nucleotides. This is also consistent with previous deletion experiments (Guerrier-Takada and Altman, 1992; Waugh and Pace, 1993; Schlegl *et al.*, 1994), indicating that the 'upper loop' region of P RNA (consisting of nucleotides 113–234 of *B.subtilis* P RNA) contributes relatively little to the formation of the P RNA active site. The inability of p(240–61) to cleave tRNA substrates is clearly due to the elimination of the binding site for the TSL motif of tRNA. By deleting the 3′ overhanging nucleotides, a variant form of P RNA, e.g. containing residues 1–396 of P RNA [p(1–396)] can be designed to cleave only pre-tRNA, but not the selected substrate. In a sense, both p(240–61) and p(1–396) represent new ribozymes specific for different RNA substrates.

Despite the presence of most, if not all, active site residues, folding analysis shows that these residues in p(240–61) are no longer folded into a structure protected from Fe(II)-EDTA cleavage (Pan, 1995a). This apparent loss in folding and retention of activity can be reconciled by two models: (i) the active site structure is not folded in the absence of substrate, but can fold in the p(240–61)–substrate complex; (ii) the active site structure is folded but has become too dynamic to provide sufficient protection against hydroxyl radical attack. Either model can explain the 20-fold lower activity of p(240–61) compared with that of the full-length P RNA toward variant #1.

The enhancement of cleavage activity by the addition of spermine demonstrates, once again, the importance of polyamines in ribozyme catalysis (Dahm and Uhlenbeck, 1991; Hanna and Szostak, 1994). Even for the tRNA substrates, the presence of spermine can effectively increase the k_{cat}/K_m of the P RNA reaction in the absence of the RNase P protein by nearly two orders of magnitude. In the case of the selected substrate, spermine appears to act at the level of the ribozyme–substrate complex, since no significant changes are present in the folding analysis of either RNA alone. However, we cannot exclude the possibility that spermine may cause subtle changes in local conformation important for the catalytic activity. This is particularly likely for p(240–61) in which tertiary folding of the active site seems to be more dynamic.

Finally, the finding of one ribozyme with two binding sites suggests an intriguing mechanism to convert RNA catalysts into multiple functional enzymes. For example, a ribozyme can use one active site to carry out catalysis but contain more than one site to bind different RNA structural motifs. Such a multiple binding site model may explain the origin of recognizing RNA substrates of diverse structures by RNase P. A ribozyme can also potentially use two binding sites to position two different substrates simultaneously into a single active site to catalyze bimolecular reactions.

Materials and methods

In vitro selection

The selection experiment was carried out as described previously (Pan, 1995b) using an RNA library containing a total of 70 randomized nucleotides. For all experiments described here, the *in vitro* transcribed p(240–61) contains a 5′ OH group after treatment with calf intestine alkaline phosphatase. Throughout the selection, the concentration of the RNA library was kept at 1 μM. In rounds 1–6 and 8, the concentration of p(240–61) was 0.4 μM and this was then reduced to 0.1 μM in rounds 7 and 9.

Characterization of selected variants

After nine cycles of selection, the cDNA of the RNA library was PCR amplified, purified, cloned and sequenced as described previously (Pan and Uhlenbeck, 1992; Pan, 1995b). The RNA of variants #1, #2 and #3 was obtained using plasmid templates purified by CsCl density gradient. To test these variants for cleavage activity, the RNAs were 5′ ^{32}P-labeled using [γ-^{32}P]ATP and polynucleotide kinase and then circularized using T4 RNA ligase. k_{cat} and K_m values for variant #1 (Table I) were determined under single turnover conditions using trace amount of ^{32}P-labeled substrate and varying concentrations of p(240–61) at 50 mM Tris–HCl, pH 8.1, 10 mM $MgCl_2$, 1 mM spermine at 37°C.

Structural mapping

RNAs were renatured by heating at 85°C for 2 min followed by incubation for 3 min at room temperature. Mg^{2+} was added to appropriate concentrations and the mixture further incubated at 37°C for 5 min.

For nuclease mapping, RNA transcripts were 5′ ^{32}P-labeled using

[γ-^{32}P]ATP and T4 polynucleotide kinase, or 3′ labeled using 5′ [^{32}P]pCp and T4 RNA ligase (England *et al.*, 1980). Reactions were performed in 50 mM Tris–HCl, pH 8.0, 10 mM $MgCl_2$ and, in some cases, 1 mM spermine. The final RNA concentration was 0.2 μM and the optimal nuclease concentrations were 0.1 U/μl T1, 0.0002 U/μl V1 and 10 U/μl S1, respectively. The cleavage reaction was carried out at 37°C for 5 min. An equal volume of a gel loading buffer containing 9 M urea/50 mM EDTA, pH 8.0 was added and the reaction products were immediately separated on 8 and 20% polyacrylamide gels containing 7 M urea.

The involvement of A, C and G residues in the secondary structure was examined by chemical modification using dimethyl sulfate (DMS, for A and C) and kethoxal (for G; Ehresmann *et al.*, 1987; Stern *et al.*, 1988). Reactions were performed in 10 μl containing 30 mM HEPES, pH 7.9, 10 mM $MgCl_2$, 2–3 pmol of RNA, 7.3 mM DMS or 150 mM kethoxal. The mixture was incubated at 37°C for 5 min. Reactions were stopped by adding 50 mM β-mercaptoethanol (for DMS) or boric acid (for kethoxal). After addition of 4 vol of 50 mM K acetate, 200 mM KCl and 1 μg of *E.coli* tRNAs, the modified RNAs were precipitated twice with ethanol. Reverse transcription of the modified RNAs was then carried out using a primer complementary to the 3′ 16 nucleotides of variant #1 as described previously (Pan, 1995b).

Acknowledgements

We thank Drs Joe Piccirilli, Kan Agarwal and one reviewer for their comments on the manuscript. This work was supported by grants from NIH (GM52993) and from CNRU at the University of Chicago (NIH DK26678). T.P. is the recipient of a Junior Faculty Research Award from the American Cancer Society (JFRA-543).

References

Altman,S., Kirsebom,L. and Talbot,S. (1993) *FASEB J.*, **7**, 7–14.
Cech,T.R. (1990) *Annu. Rev. Biochem.*, **59**, 543–568.
Cech,T.R. (1993) In Gesteland,R. and Atkins,J. (eds), *The RNA World*. Cold Spring Harbor Laboratory Press, Cold Spring Harbor, NY, pp. 239–269.
Dahm,S.C. and Uhlenbeck,O.C. (1991) *Biochemistry*, **30**, 9464–9469.
Doudna,J.A. and Cech,T.R. (1995) *RNA*, **1**, 36–45.
Doudna,J.A. and Szostak,J.W. (1989) *Nature*, **339**, 519–522.
Ehresmann,C., Baudin,F., Mougel,M., Romby,P., Ebel,J.-P. and Ehresmann,B. (1987) *Nucleic Acids Res.*, **15**, 9109–9128.
England,T.E., Bruce,A.G. and Uhlenbeck,O.C. (1980) *Methods Enzymol.*, **65**, 65–75.
Forster,A.C. and Altman,S. (1990) *Science*, **249**, 783–786.
Guerrier-Takada,C. and Altman,S. (1992) *Proc. Natl Acad. Sci. USA*, **89**, 1266–1270.
Haas,E.S., Brown,J.W., Pitulle,C. and Pace,N.R. (1994) *Proc. Natl Acad. Sci. USA*, **91**, 2527–2531.
Hanna,M. and Szostak,J.W. (1994) *Nucleic Acids Res.*, **22**, 5326–5331.
Harris,M.E., Nolan,J.M., Malhotra,A., Brown,J.W., Harvey,S.C. and Pace,N.R. (1994) *EMBO J.*, **13**, 3953–3963.
Hartmann,R.K., Heinrich,J., Schlegl,J. and Schuster,H. (1995) *Proc. Natl Acad. Sci. USA*, **92**, 5822–5826.
Kirsebom,L.A. and Svard,S.G. (1994) *EMBO J.*, **13**, 4870–4876.
Komine,Y., Kitabatake,M., Yokogawa,T., Nishikawa,K. and Inokuchi,H. (1994) *Proc. Natl Acad. Sci. USA*, **91**, 9223–9227.
LaGrandeur,T.E., Huttenhofer,A., Noller,H.F. and Pace,N.R. (1994) *EMBO J.*, **13**, 3945–3952.
Long,D.M. and Uhlenbeck,O.C. (1993) *FASEB J.*, **7**, 25–30.
Nolan,J.M., Burke,D.H. and Pace,N.R. (1993) *Science*, **261**, 762–765.
Oh,B.-K. and Pace,N.R. (1994) *Nucleic Acids Res.*, **22**, 4087–4094.
Pace,N.R. and Brown,J.W. (1995) *J. Bacteriol.*, **177**, 1919–1928.
Pan,T. (1995a) *Biochemistry*, **34**, 902–909.
Pan,T. (1995b) *Biochemistry*, **34**, 8458–8464.
Pan,T. and Uhlenbeck,O.C. (1992) *Biochemistry*, **31**, 3887–3895.
Pan,T., Loria,A. and Zhong,K. (1995) *Proc. Natl Acad. Sci. USA*, **92**, 12510–12514.
Peck-Miller,K.A. and Altman,S. (1991) *J. Mol. Biol.*, **221**, 1–5.
Schlegl,J., Hardt,W.-D., Erdmann,V. and Hartmann,R.K. (1994) *EMBO J.*, **13**, 4863–4869.
Stern,S., Moazed,D. and Noller,H.F. (1988) *Methods Enzymol.*, **164**, 481–489.
Talbot,S.J. and Altman,S. (1994) *Biochemistry*, **33**, 1399–1405.
Turner,D.H., Sugimoto,N. and Freier,S.M. (1988) *Annu. Rev. Biophys. Biophys. Chem.*, **17**, 167–192.
Waugh,D.S. and Pace,N.R. (1993) *FASEB J.*, **7**, 188–195.
Westhof,E. and Altman,S. (1994) *Proc. Natl Acad. Sci. USA*, **91**, 5133–5137.
Wyatt,J.R., Puglisi,J.D. and Tinoco,I.,Jr (1990) *J. Mol. Biol.*, **214**, 455–470.

Received on December 7, 1995; revised on January 15, 1996